Supporting Information for:

Directing Nanoparticle Biodistribution Through Evasion and Exploitation of Stab2-Dependent Nanoparticle Uptake

Frederick Campbell[a*], Frank L. Bos[b,#,&], Sandro Sieber[c,&], Gabriela Arias-Alpizar[a,&], Bjørn E. Koch[d], Jörg Huwyler[c], Alexander Kros[a*] and Jeroen Bussmann[a,d*]

[a]Department of Supramolecular & Biomaterials Chemistry, Leiden Institute of Chemistry (LIC), Leiden University, P.O. Box 9502, 2300 RA Leiden, The Netherlands

[b]Hubrecht-Institute-KNAW and University Medical Centre and Centre for Biomedical Genetics, Uppsalalaan 8, 3584 CT, Utrecht, The Netherlands.

[c]Division of Pharmaceutical Technology, Department of Pharmaceutical Science, University of Basel, Klingelbergstrasse 50, Basel CH-4056, Switzerland

[d]Department of Molecular Cell Biology, Institute Biology Leiden (IBL), Leiden University, P.O. Box 9502, 2300 RA Leiden, The Netherlands

[#]Current affiliation: Princess Máxima Center for Pediatric Oncology, Utrecht 3584CT, The Netherlands.

[&]These authors contributed equally

* Corresponding authors. E-mail: j.bussmann@chem.leidenuniv.nl; a.kros@chem.leidenuniv.nl; f.campbell@chem.leidenuniv.nl

Table of Contents

Supporting Methods

Reagents

1,2-dioleoyl-*sn*-glycero-3-phosphocholine (DOPC), 1,2-distearoyl-*sn*-glycero-3-phosphocholine (DSPC), 1,2-dioleoyl-*sn*-glycero-3-phospho-(1'-*rac*-glycerol) (DOPG), 1,2-distearoyl-*sn*-glycero-3-phospho-(1'-*rac*-glycerol) (DSPG), 1-palmitoyl-2-oleoyl-*sn*-glycero-3-phosphocholine (POPC), 1,2-dioleoyl-*sn*-glycero-3-phospho-L-serine (sodium salt) (DOPS), 1,2-dioleoyl-3-trimethylammonium-propane (DOTAP), 1,2-dioleoyl-*sn*-glycero-3-phosphoethanolamine-N-[methoxy(polyethylene glycol)-2000] (DOPE-mPEG2000), 1,2-dioleoyl-*sn*-glycero-3-phosphoethanolamine-N-(lissamine rhodamine B sulfonyl) (Rhodamine-PE) were purchased from Avanti Polar Lipids (Alabaster, US). 1,2-Dioleoyl-*sn*-glycero-3-phosphoethanolamine-Atto 633 was purchased from ATTO-TEC GmbH (Germany). Additional DOPC and DSPC were purchased from Lipoid GmbH. Additional POPC and cholesterol was purchased from Sigma-Aldrich. All solvents were purchased from Biosolve Ltd. Dichloromethylenediphosphonic acid disodium salt (clodronic acid), carminic acid and dextran sulfate (40kDa) were purchased from Sigma-Aldrich. Hyaluronic acid (sodium salt, 100kDa) was purchased from Lifecore Biomedical Inc. Quantum dots (Qdot 605 ITK carboxyl) and oxidized low density lipoprotein (oxLDL from human plasma, DiI conjugate) were purchased from Thermo Fisher. 100nm red fluorescent polystyrene, sulfate modified nanoparticles ('latex beads') were purchased from Sigma Aldrich.

Size and zeta potential measurements

Particle size and zeta potentials were measured using a Malvern Zetasizer Nano ZS. For DLS, measurements were carried out at room temperature in ddH_20 at a total lipid concentration of 100μM. For zeta potential measurements, liposome solutions were first diluted in salt (NaCl) solution. Zeta potentials were measured at room temperature, at 500μM total lipid concentration and 10mM NaCl concentration. All reported DLS measurements and zeta potentials are the average of three measurements.

Image quantification

First, average intravascular fluorescence within the dorsal aorta (DA) was measured within an ~8um*10um rectangular area (~$1*10^3$ pixels) in a single confocal slice that captured the center of the DA (Extended Data Figure 2-I). This measurement was repeated three times per embryo in independent sites within the DA. Second, total fluorescence and total vasculature associated fluorescence was quantified using the following ImageJ macro:

ImageJ quantification macro

```
rename("stack");
run("Z Project...", "projection=[Max Intensity]");
run("Split Channels");
selectWindow("C2-MAX_stack");
close();
selectWindow("C1-MAX_stack");
run("Duplicate...", "title=vascular");
selectWindow("vascular");
setThreshold(5, 255);
run("Convert to Mask");
run("Invert LUT");
run("Subtract...", "value=254");
run("Duplicate...", "title=nonvascular");
run("Macro...", "code=v=abs(v-1)");
imageCalculator("Multiply create", "vascular","C3-MAX_stack");
imageCalculator("Multiply create", "nonvascular","C3-MAX_stack");
selectWindow("C3-MAX_stack");
run("Measure");
selectWindow("Result of vascular");
run("Measure");
run("Concatenate...", "  title=[Concatenated Stacks] keep image1=C1-MAX_stack
image2=[Result of nonvascular] image3=[Result of vascular] image4=[-- None --]");
```

Finally, the angle of the dorsal aspect of the dorsal aorta (a straight line) was measured and the concatenated images were rotated to orient the dorsal aorta horizontally within the image. Images were subsequently cropped to a rectangle encompassing the caudal vein, DA or the area between the DA and the dorsal longitudinal anastomotic vessel (DLAV) to quantify the vasculature-associated fluorescence associated with veins (caudal vein) and arteries (DA), as well as the extravascular fluorescence around the intersegmental vessels (Extended Data Figure 2-III). The latter area was used to quantify extravascular fluorescence since it does not contain pigment cells that are present on the dorsal and ventral side of the embryo and which are autofluorescent within the rhodamine-PE channel. Although the CHT endothelial cells appear to behave very similar to the CV endothelial cells, quantification was performed based on the CV alone for the following reasons. First, the CV is always perfused, whereas perfusion of the vessels within the CHT is variable. Unperfused or weakly perfused vessels display absence of or reduced nanoparticle uptake. Secondly, variable numbers of hematopoietic cells - especially macrophages - are closely associated with CHT-ECs and much less with the CV. Macrophage uptake of nanoparticles could therefore lead to the false impression that CHT-ECs selectively take up nanoparticles.

From these data, the following measures were reported:

1. Average intravascular fluorescence (Figure 1e, Extended Data Figure 4b)
2. Venous/Arterial (Figure 1f, 3a,b,f-k, 4a-j,m, Extended Data Figure 4d):
   (Mean CV fluorescence/%GFP positive within CV area)/(Mean DA fluorescence/%GFP positive within DA area)
3. Extravascular (Figure 1g, Extended Data Figure 4c): Extravascular fluorescence/%GFP negative within ISV area
4. Vessel wall/Intravenous (Figure 1h, Extended Data Figure 4e): (Total vascular fluorescence/%GFP positive within the total image)/Average intravascular fluorescence

Table S1. Nanoparticle composition, size and zeta potential. For liposomes, size and polydispersity (PDI) ranges correspond to a least three independent formulations, with the exception of:
[a.] The sizes of both 'Myocet 325nm' and 'Myocet 465nm' liposomes varied significantly batch to batch. The size, PDI and zeta potentials reported for these formulations relate to those for which data is presented in Extended Data Figure 2.
[b.] Data for two independent formulations.
[c.] Zeta potential for unmodified (ie. no conjugated dye) CCMV VLPs (t=3)
[b.] Data for two independent formulations only.

Formulation	Composition*	Size/nm	PDI	Zeta Potential/mV
Myocet	POPC:Cholesterol (55:45)	114.5 - 122.1	0.04 - 0.06	-15.8
AmBisome	DSPC:DSPG:Cholesterol (53:21:26)	118.8 - 133.7	0.05 - 0.07	-33.7
EndoTAG-1	DOTAP:DOPC (51.5:48.5)	109.6 - 114.3	0.03 - 0.05	+46.0
Myocet (325nm)	POPC:Cholesterol (55:45)	325.4[a]	0.22	-18.6
Myocet (465nm)	POPC:Cholesterol (55:45)	464.5[a]	0.24	-20.0
Myocet + PEG	POPC:Cholesterol:DOPE-mPEG2000 (50:41:9)	100.4 - 118.0	0.05 - 0.06	-11.8
100% DOPC	DOPC	114.8 - 118.4	0.07 - 0.09	-11.3
100% DSPC	DSPC	102.0 - 108.3	0.06 - 0.07	-3.4
100% DOPG	DOPG	114.0 - 121.8	0.03 - 0.07	-37.1
100% DSPG	DSPG	95.4 - 102.9	0.12 - 0.17	-45.9
100% DOTAP	DOTAP	101.8 - 114.8[b]	0.06 - 0.07	+35.6
100% POPC	POPC	108.0 - 111.4	0.07 - 0.08	-17.2
Polymersomes	PIB:PEG (1:0.75 mol ratio)	83.0	0.26	-24.0
Virus-like particles	90 CCMV capsid protein dimers	28.0	ND	-14.9[c]
Quantum Dots	CdSe core:ZnS shell:n-octylamine-modified poly acrylic acid (PnOAm-co-PAA) copolymer cap	≈ 5 x 12 (by TEM)	ND	-70.8
Latex beads	carboxylate-modified polystyrene	121.4	0.02	-51.0
* all lipsome formulations + 1mol% DOPE-LR/+1mol% DOPE-Atto633				

Table S2. Liposome composition, size and encapsulated clodronic acid.
[a.] Data for three seperate formulations

Formulation	Lipid Composition	Size/nm	PDI	Encapsulated Clodronate/ mgmL^{-1}
100% DOPC	DOPC	126.6	0.07	0.9
100% DSPC	DSPC	128.3 - 132.2[a]	0.06 - 0.09	1.21 - 1.72

Table S3. Guide RNA sequences and primers.

Gene	Sequences (F: Forward, R: Reverse)
Stabilin1	
sgRNA	TAATACGACTCACTATAGGATCTGATGACTCCATTCCGTTTTAGAGCTAGAAATAGC
Genotyping	**F**: TGTAAAACGACGGCCAGTCACCACCTGTGAACTCATAAGC
	R: GTGTCTTCGTTATCATTCAGGAAACAGCA
In Situ hybridisation	**F**: GAGGTTGCCATGAAGAAGCCGAC
	R: GCAACAACCGAAGCCAAGTCTCC
Stabilin2	
sgRNA	TAATACGACTCACTATAGGCACACACTCCTCAAGCACGTTTTAGAGCTAGAAATAGC
Genotyping	**F:** TGTAAAACGACGGCCAGTCCTTTTTGAACTCACAAATGCTC
	R: GTGTCTTGTCATACACACAGCGGGTAGAG
In Situ hybridisation	**F:** CGCCTTCGGAACATCACTATCCAG
	R: CCTGCAGGAGCTCAAAGACTCCAC
Mrc1a	
In Situ hybridisation	**F:** TGTGGACTGATGGTAAAGGTGTCAGC
	R: CTCAGGACAGTTCCCTGGCATCTG

Supporting Movie and Figure Legends

Movie 1. An uninjected control embryo and three DSPC-clodronic acid (10mM total lipids) liposome injected embryos showing blood flow dynamics in the tail region and normal embryonic development 48h after injection. Black arrows indicate the most caudal end of the PCV that contains bloodflow, white arrows indicate the most caudal perfused ISV.

Movie 2. Timelapse confocal imaging of a *kdrl:GFP* transgenic embryo injected with DSPC-clodronic acid (10mM total lipids) liposome. Imaging started 6hpi. Confocal z-stacks were captured every 20 minutes for 24 hours.

Movie 3. Three sibling control embryo and three *stab2*^{ibl2} homozygous mutants DSPC-clodronic acid (10mM total lipids) liposome injected embryos showing blood flow dynamics in the tail region and normal embryonic development 48h after injection.

Figure S1. Confocal images of individual embryos that were used for image quantification. Twelve (n=12) cellular views of Myocet, AmBisome and EndoTAG-1 liposome distribution in *kdrl:GFP* transgenic zebrafish embryos at 1,8, 24 and 48hpi. For Myocet 48hpi, n=11, and for EndoTAG-1 24hpi and 48hpi, n=6.

Figure S2. Overview of quantification method as described in the Materials & Methods section. I. Quantification of intravascular fluorescence (liposomes in circulation). **II.** Quantification of total and total vascular fluorescence. **III.** Quantification of arterial, venous and extravascular fluorescence.

Figure S3. Size-dependent uptake of neutral liposomes by monocytes/macrophages. A. Whole-embryo and cellular views of liposome distribution in *mpeg:GFP* transgenic embryos, 2h after injection with Myocet liposomes ~100nm (with and without 10 mol% DOPE-mPEG2000), 325nm and 464nm pores. Immobile liposome aggregates were observed to colocalize with *mpeg:gfp* positive macrophages/monocytes within the caudal hematopoietic tissue (CHT). Fluorescence intensity was found to increase with increased liposome size, and phagocytosis could be prevented by PEGylation. **B.** High-resolution imaging shows intracellular localization of 400nm liposomes within macrophages/monocytes.

Figure S4. Contribution of individual lipids to liposome biodistribution. A. Cellular view of liposome distribution in *kdrl:GFP* transgenic embryos, 1h and 8h after injection with liposomes generated from six different individual lipids. **B.** Quantification of liposome levels in circulation based on rhodamine fluorescence intensity in the lumen of the dorsal aorta at 1h after injection. **C.** Quantification of extravascular liposome levels based on rhodamine fluorescence intensity outside of the vasculature between the DLAV and DA at 8h after injection. **D.** Quantification of liposome levels associated with venous vs. arterial endothelial cells based on rhodamine fluorescence intensity associated with caudal vein vs. DA at 8h after injection. **E.** Quantification of liposome levels associated with the vessel wall based on relative rhodamine fluorescence intensity associated with all endothelial cells vs. rhodamine fluorescence intensity in circulation at 1h after injection. **B-E.** Bar height represents median values, dots represent individual data points, significantly different pairs of values based on Kruskal-Wallis and Dunn's test with Bonferroni correction are indicated by colored boxes (representing significance levels; CV=critical value; NT=not tested). n=6 individually injected embryos per group (in 2 experiments).

Figure S5. Macrophage uptake of DOPG and DSPC liposomes. Confocal micrographs of *kdrl:GFP* (green)*; mpeg:RFP* (red) double transgenic embryos injected with DOPE-ATTO633 labeled DOPG (**A**) or DSPC (**B**) liposomes. Besides uptake of liposomes in caudal vein (CV, brackets) endothelial cells, uptake by plasma-exposed (arrowheads) but not extravascular (asterisks) macrophages/monocytes is also observed for both liposomes

Figure S6. Expression of LSEC marker genes in zebrafish embryos A,B. Whole-mount *in situ* hybridization of *stab1, stab2* and *mrc1a* mRNA. **A.** Whole-embryo view showing expression of these genes in the PHS, CCV, PCV and CV **B.** Higher-resolution image showing expression in the entire caudal vein, but only on the dorsal side of the PCV (arrows).

Figure S7. FluoHA colocalization with liposomes. A,B. Whole-embryo view of coinjected fluoHA (green) and **A.** DOPG liposomes or **B.** DSPC liposomes (red), 1h after injection, reveals colocalization in PHS, CCV, PCV and CV scavenger endothelial cells. **C.** Tissue level view of coinjected fluoHA and DOPG liposomes, 1h after injection reveals colocalization in SECs. Monocytes/macrophages (arrowheads) take up DSPC but not fluoHA. **D.** Cellular view of coinjected fluoHA (green) and DOPG or DSPC liposomes (blue) in *mpeg:RFP* (red) transgenic embryos. Colocalization of fluoHA with both liposomes is observed in all SECs, but not in macrophages/monocytes, which only take up liposomes, but not fluoHA.

Figure S8. FluoHA distribution through embryonic development. A. Whole-embryo view of fluorescent hyaluronic acid (fluoHA) distribution in *kdrl:RFP* transgenic embryos, 1h after injection. SECs, as identified through intracellular accumulation of fluoHA from 28hpf to at least 128hpf. From 104hpf, fluoHA uptake is also observed in lymphatic vessels, such as the thoracic duct (TD) and facial lymphatics (FL) **B.** Cellular view of fluoHA distribution in the trunk of *kdrl:RFP* transgenic embryos, 1h after injection. A gradual restriction of fluoHA accumulation to the PCV is observed between 52hpf and 104hpf.

Figure S9. CRISPR/Cas9 induced mutations. A. Nucleotide sequences surrounding the CRISPR/Cas9 targeting sites in the *stab2*^{ibl2} allele. Protospacer Adjecent Motif (PAM) sequences are indicated in red, sgRNA target sites are indicated in green, arrows indicate the predicted Cas9 cutting site. A silent single-nucleotide polymorphism (C->T, red) was also identified in the *stab2*^{ibl2} allele. **B.** Predicted amino acid sequences surrounding the CRISPR/Cas9 targeting sites in the *stab2*^{ibl2} allele. Frameshift-induced amino acids and stop codons are indicated in red.

Figure S10. Gene expression in *stab2*^{ibl2} homozygous mutant embryos. Whole-mount *in situ* hybridization of *stab1* and *mrc1* mRNA expression at 56hpf and *stab2* mRNA expression at 32hpf and 56hpf in the trunk and tail of *stab2*^{ibl2} homozyogous mutant and sibling control embryos. A reduction in *stab2* expression indicating nonsense-mediated decay of the *stab2*^{ibl2} mRNA is observed *stab2*^{ibl2} homozygous, but not sibling control embryos. Expression of *stab1* and *mrc1* is unchanged indicating normal SEC differentiation.

Figure S11. Clonal *stab2* deletion. Whole-embryo and cellular views of DOPG liposome distribution in *stab2*$^{ibl2/+}$; *kdrl:GFP*$^{+}$ embryos. CRISPR/Cas9 introduced mutations in the wildtype allele generated clones of cells without *stab2* function. In *stab2 sgRNA* and *Cas9* mRNA injected, but not control embryos, endothelial cell clones are observed in which DOPG accumulation is abrogated, indicating a requirement for *stab2* function within SECs.

Figure S12. Cell-type selectivity of DSPC-clodronic acid liposomes. Confocal imaging of *mpeg:GFP* (macrophage/monocytes) and *mpx:GFP* (neutrophil) transgenic zebrafish embryos 48h after injection with 1nl of DSPC-clodronic acid liposomes (10mM total lipids) showing normal development of these lineages in the tail of injected embryos compared to uninjected controls (UIC).

Figure S1

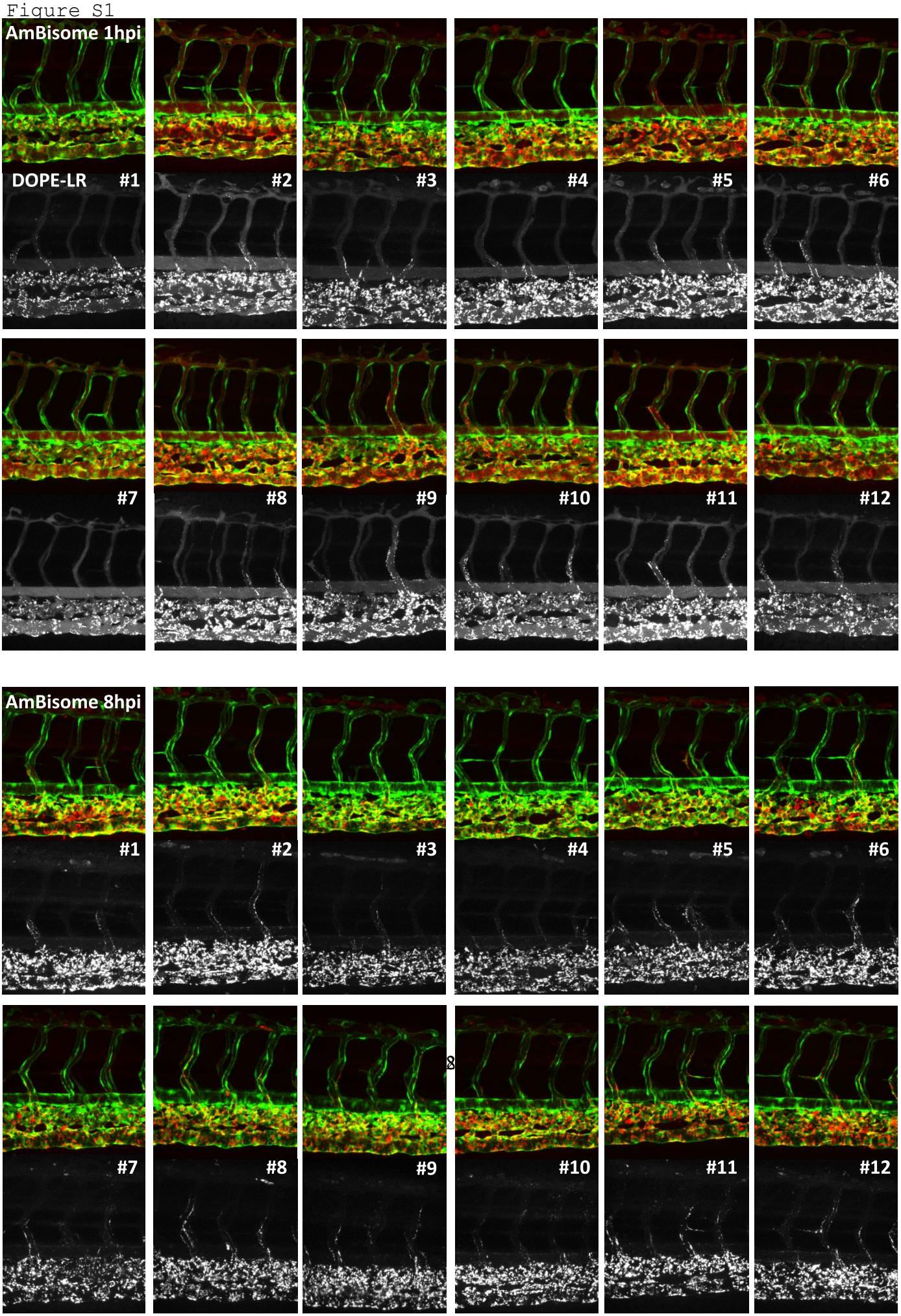
AmBisome 1hpi
DOPE-LR
#1
#2
#3
#4
#5
#6
#7
#8
#9
#10
#11
#12
AmBisome 8hpi
#1
#2
#3
#4
#5
#6
#7
#8
#9
#10
#11
#12

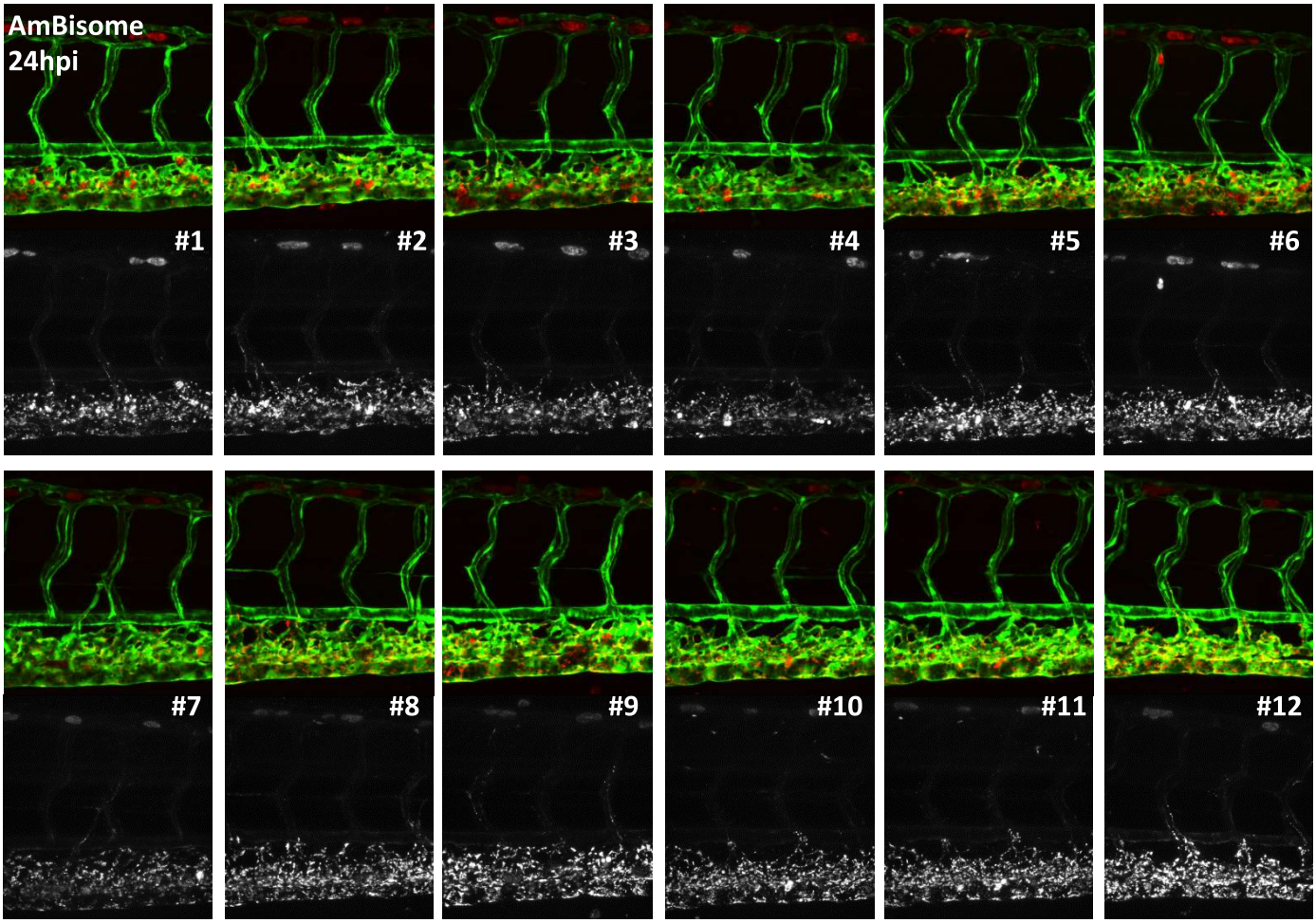
AmBisome
24hpi
#1
#2
#3
#4
#5
#6
#7
#8
#9
#10
#11
#12

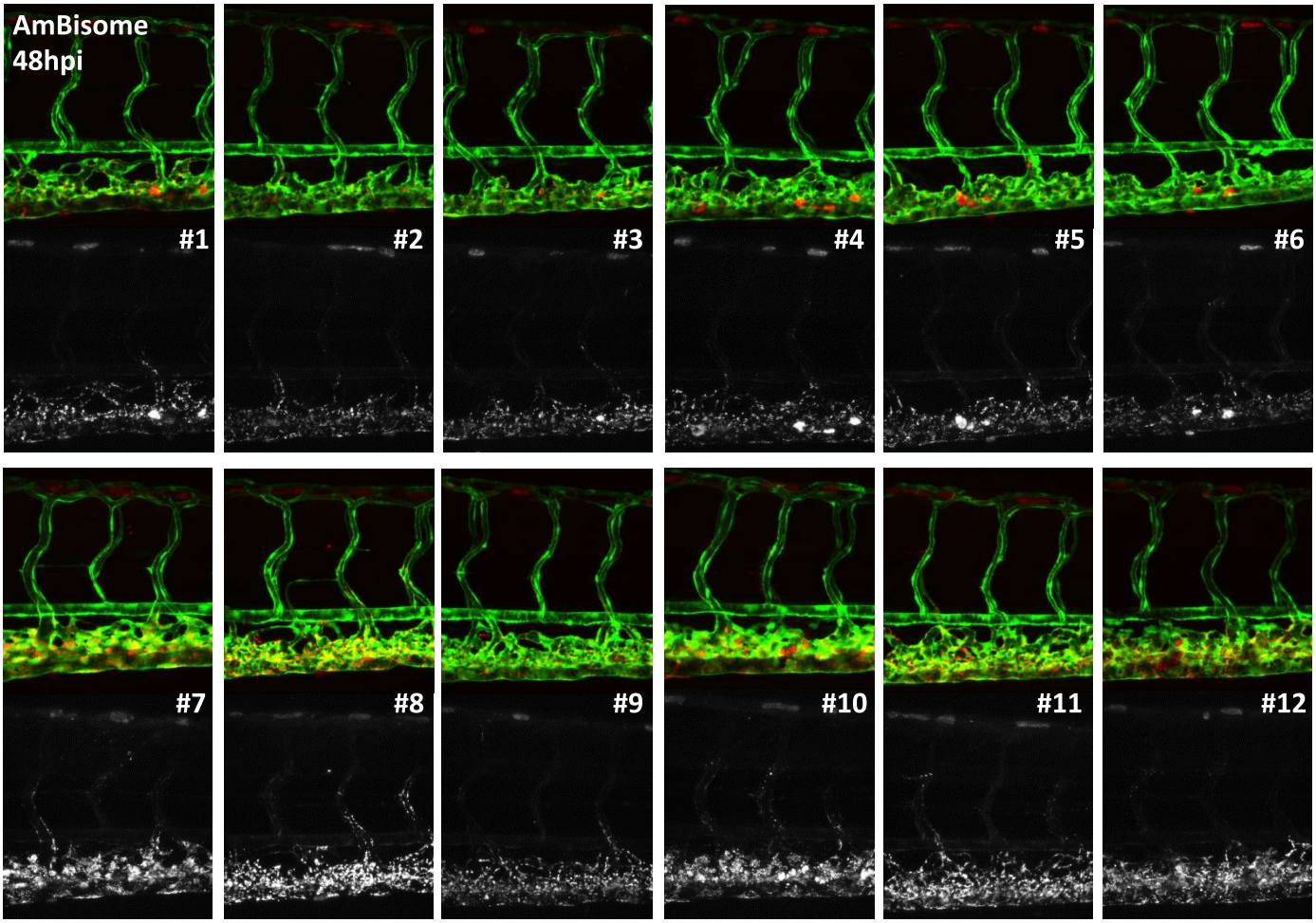
AmBisome
48hpi
#1
#2
#3
#4
#5
#6
#7
#8
#9
#10
#11
#12

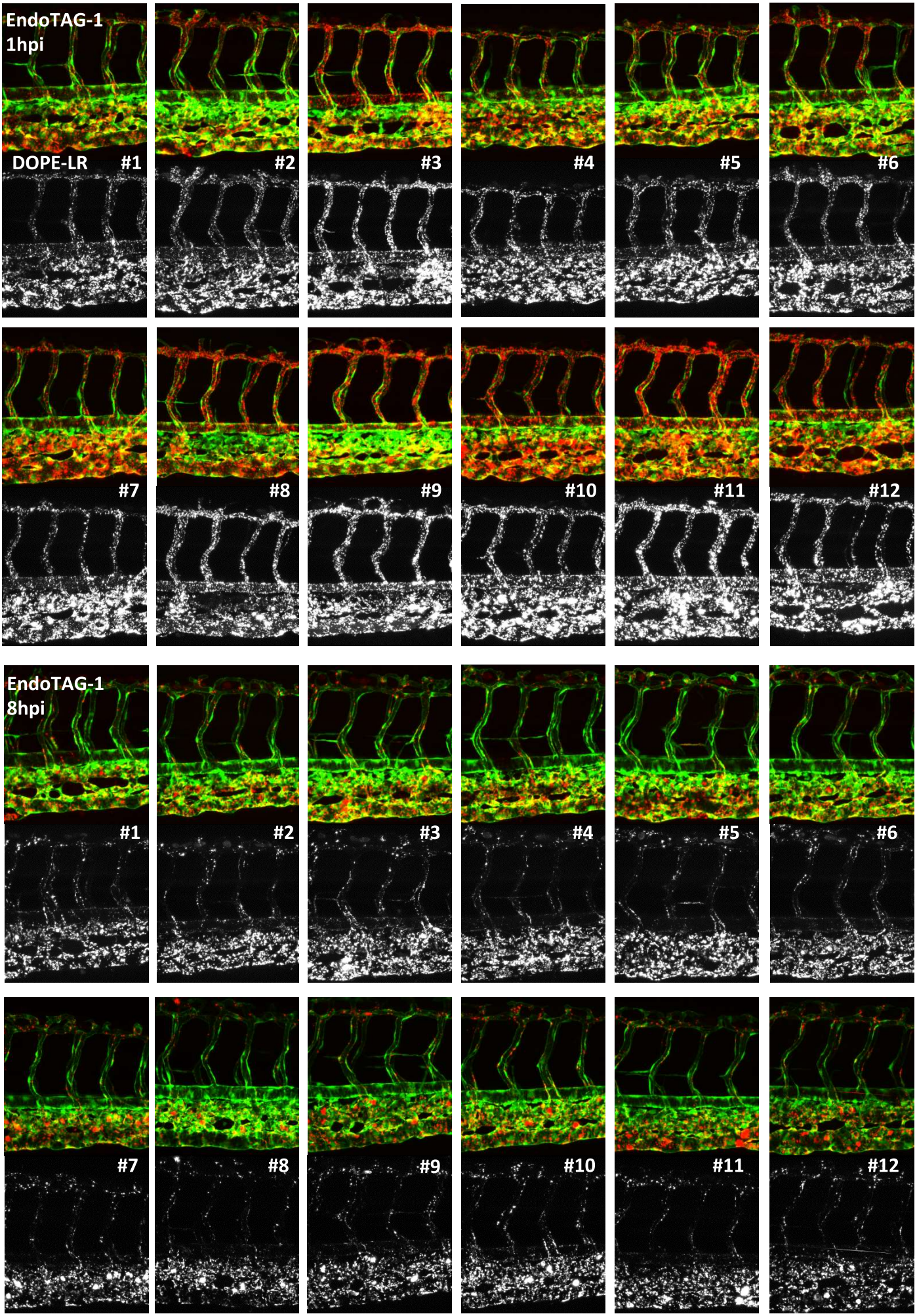
EndoTAG-1
1hpi
DOPE-LR
#1
#2
#3
#4
#5
#6
#7
#8
#9
#10
#11
#12
EndoTAG-1
8hpi
#1
#2
#3
#4
#5
#6
#7
#8
#9
#10
#11
#12

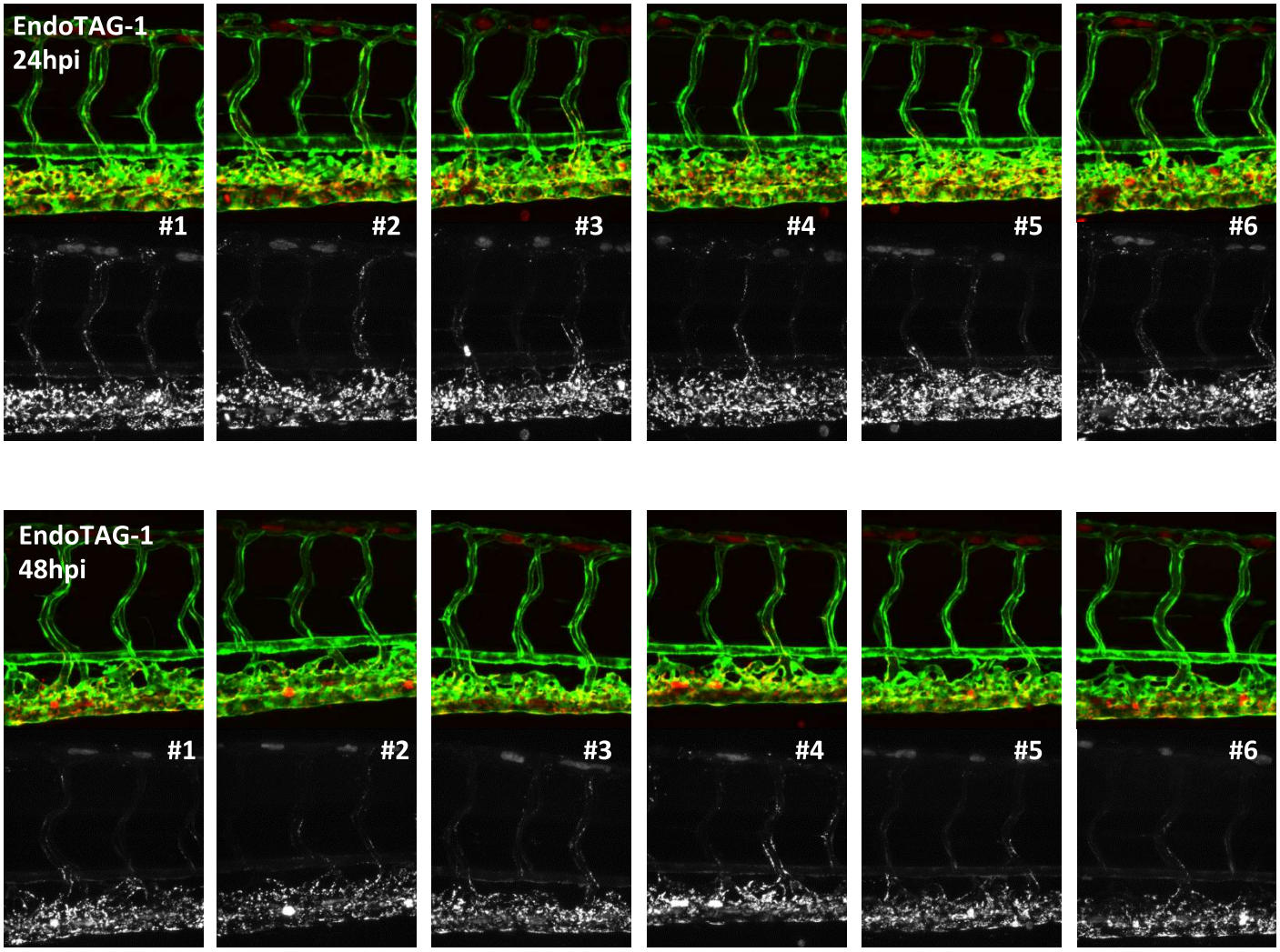
EndoTAG-1
24hpi
#1
#2
#3
#4
#5
#6
EndoTAG-1
48hpi
#1
#2
#3
#4
#5
#6

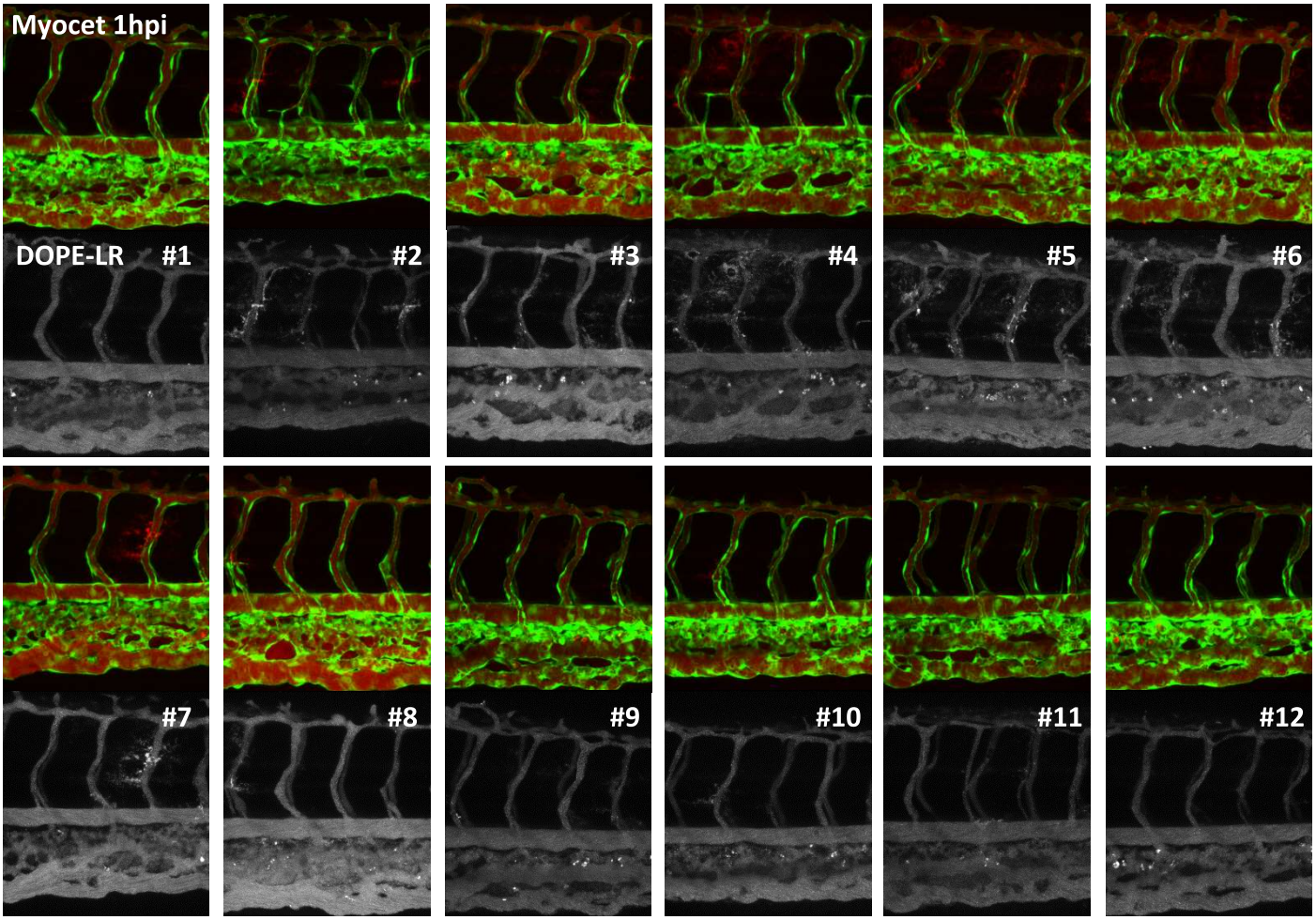
Myocet 1hpi
DOPE-LR
#1
#2
#3
#4
#5
#6
#7
#8
#9
#10
#11
#12

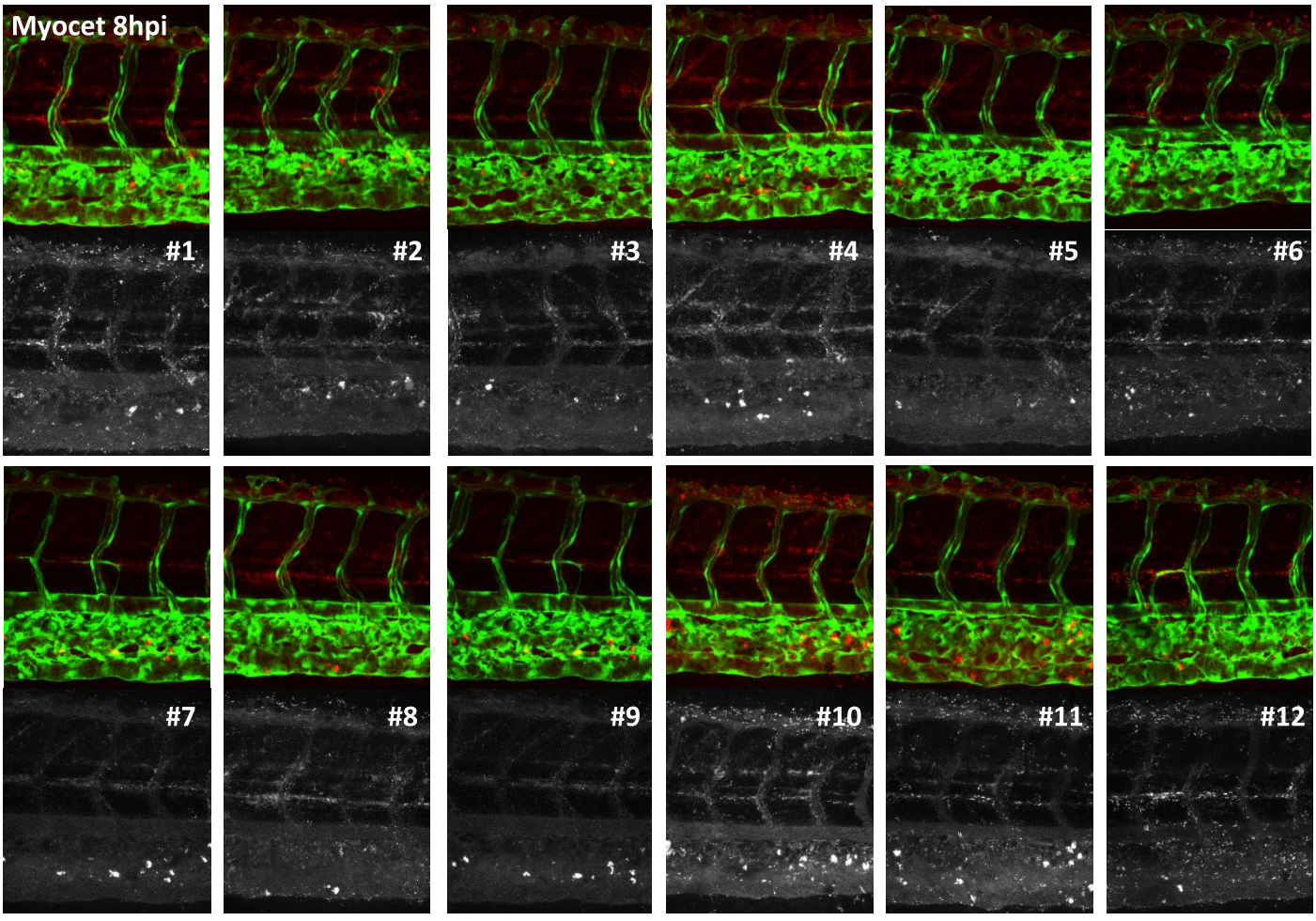
Myocet 8hpi
#1
#2
#3
#4
#5
#6
#7
#8
#9
#10
#11
#12

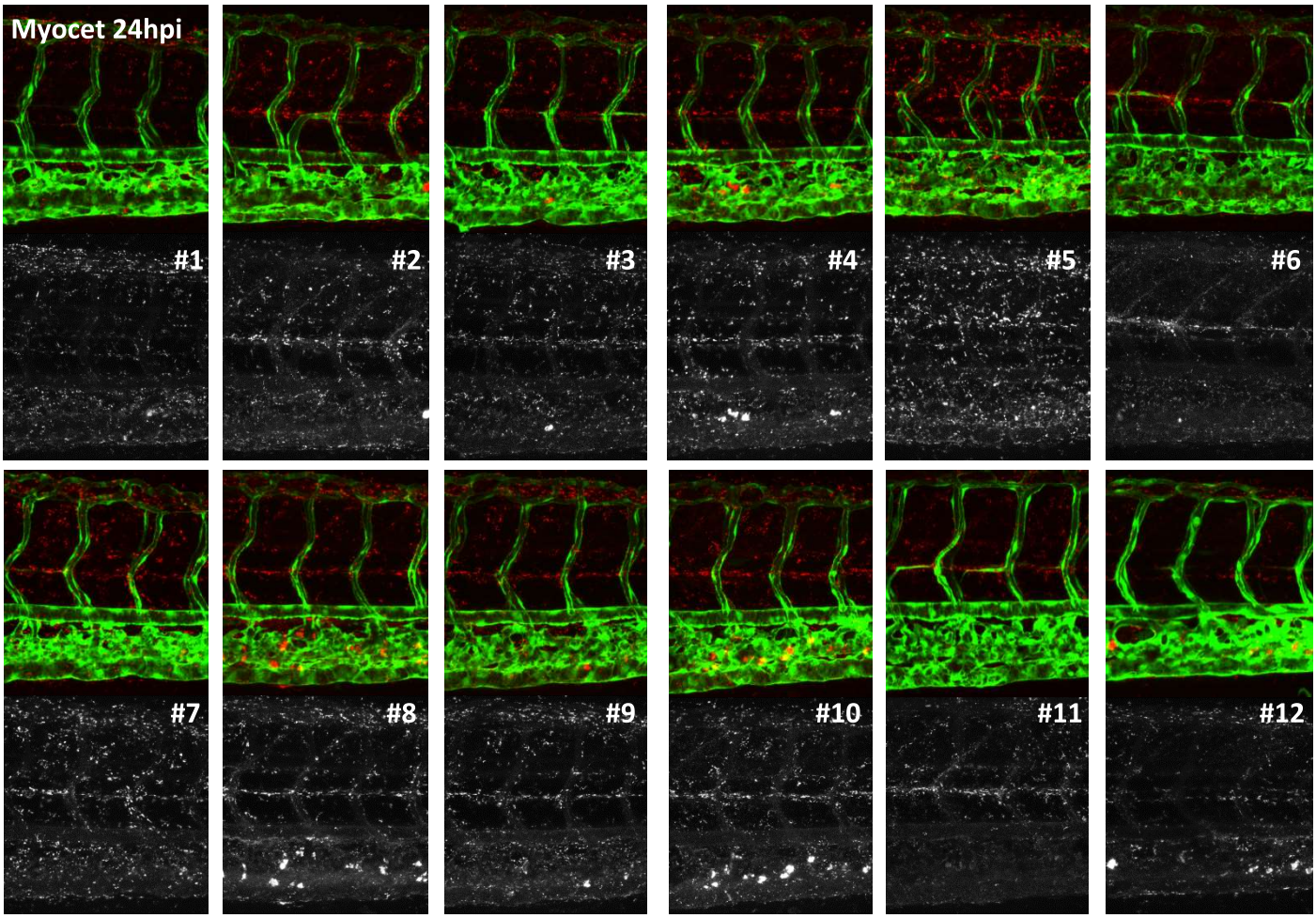
Myocet 24hpi
#1
#2
#3
#4
#5
#6
#7
#8
#9
#10
#11
#12

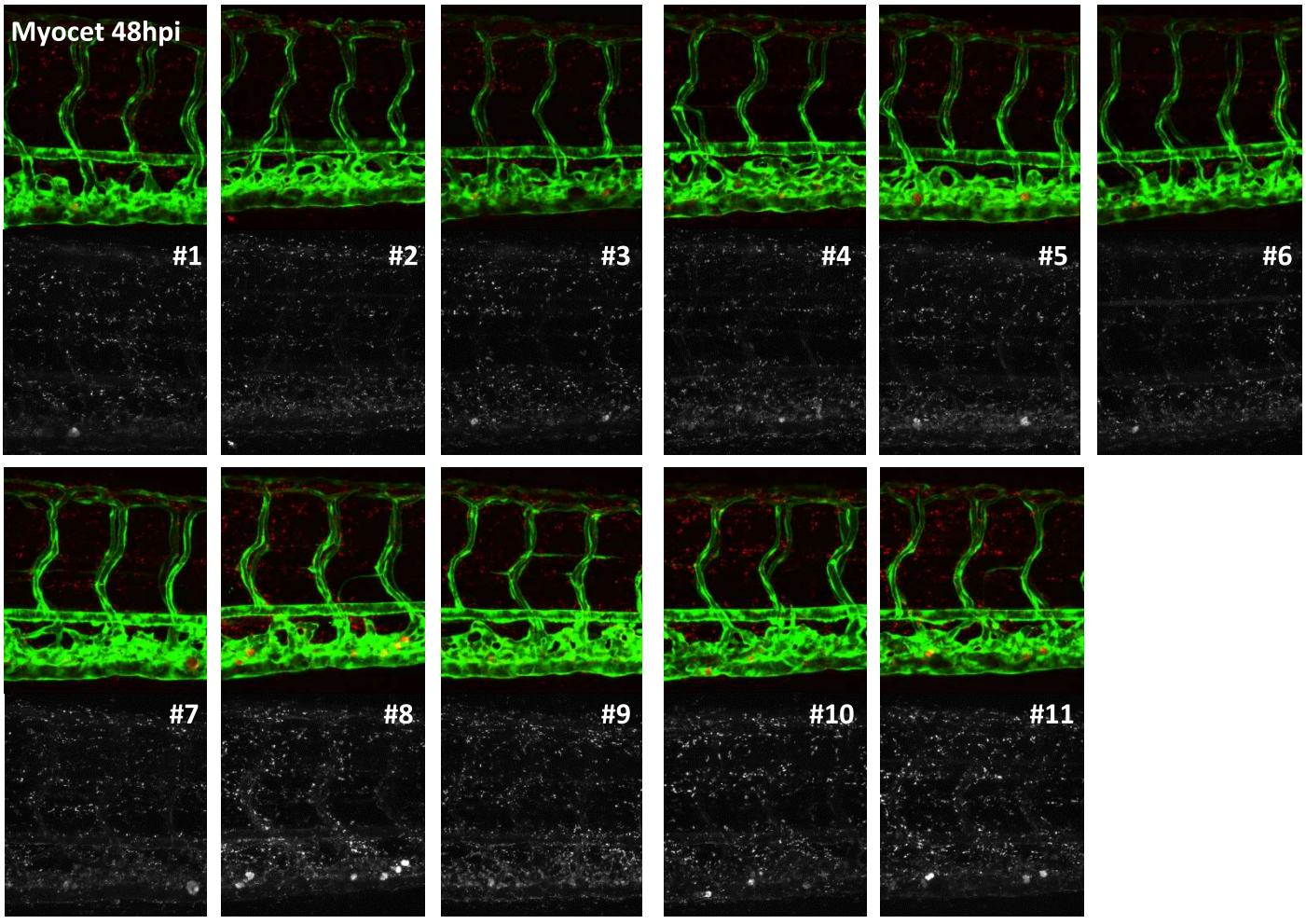
Myocet 48hpi
#1
#2
#3
#4
#5
#6
#7
#8
#9
#10
#11

Figure S2

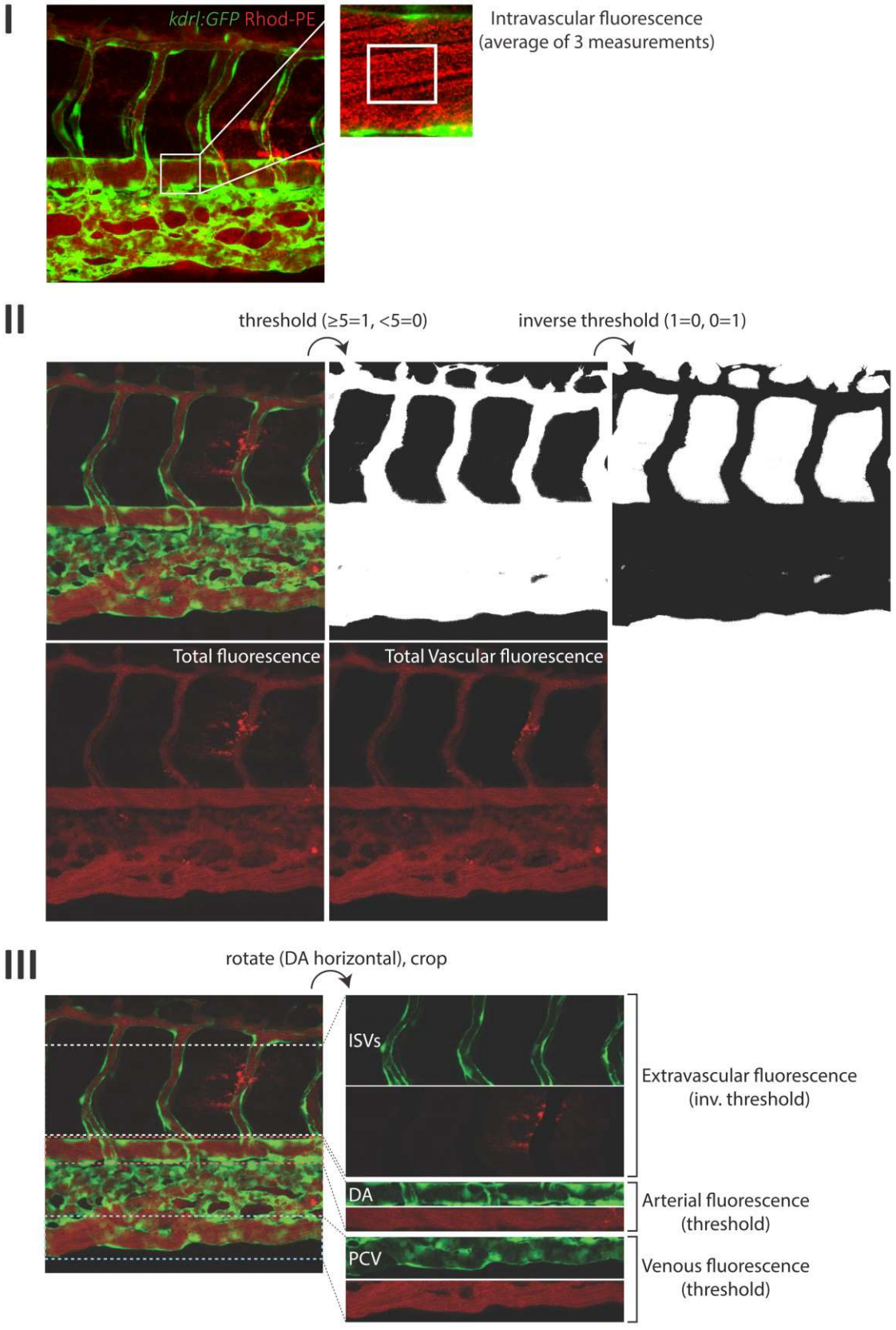
I
kdrl:GFP Rhod-PE
Intravascular fluorescence
(average of 3 measurements)
II
threshold (≥5=1, <5=0)
inverse threshold (1=0, 0=1)
Total fluorescence
Total Vascular fluorescence
III
rotate (DA horizontal), crop
ISVs
DA
PCV
Extravascular fluorescence
(inv. threshold)
Arterial fluorescence
(threshold)
Venous fluorescence
(threshold)

Figure S3

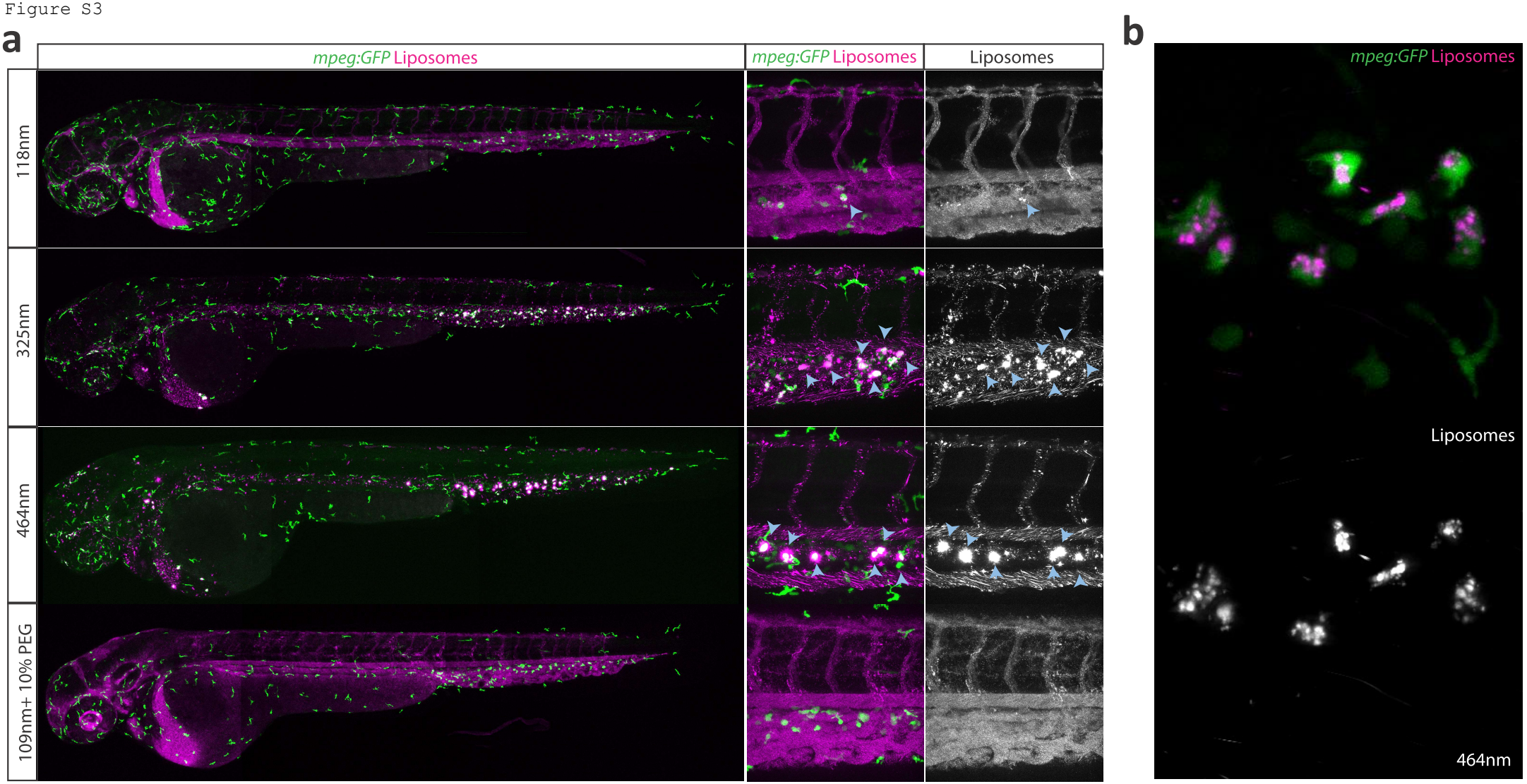
a
mpeg:GFP Liposomes
mpeg:GFP Liposomes
Liposomes
118nm
325nm
464nm
109nm+ 10% PEG
b
mpeg:GFP Liposomes
Liposomes
464nm

Figure S4

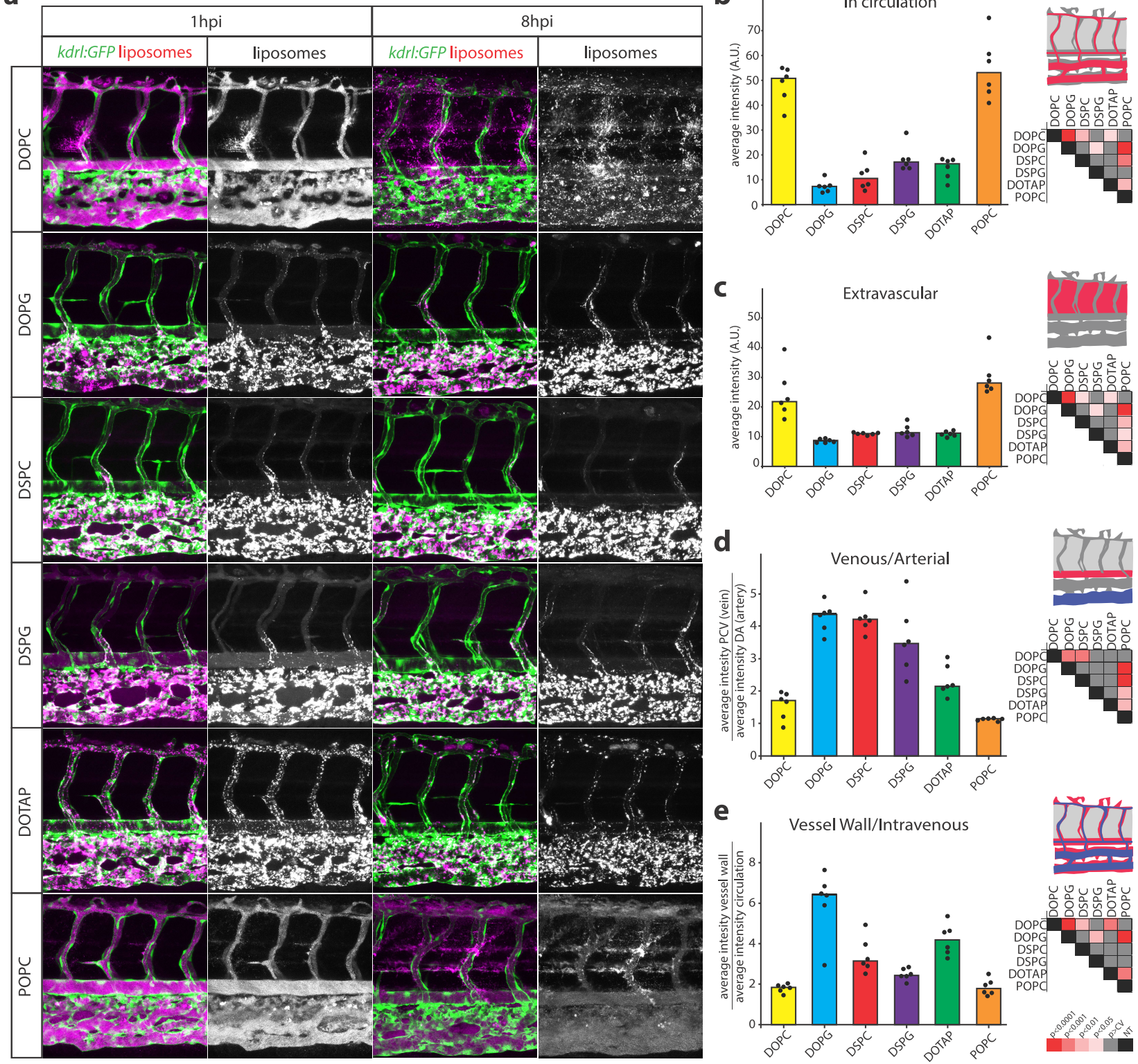
a
1hpi
8hpi
kdrl:GFP liposomes
liposomes
kdrl:GFP liposomes
liposomes
DOPC
DOPG
DSPC
DSPG
DOTAP
POPC
b
In circulation
average intensity (A.U.)
c
Extravascular
average intensity (A.U.)
d
Venous/Arterial
average intesity PCV (vein)
average intensity DA (artery)
e
Vessel Wall/Intravenous
average intesity vessel wall
average intensity circulation
p<0.0001
p<0.001
p<0.01
p<0.05
p>CV
NT

Figure S5

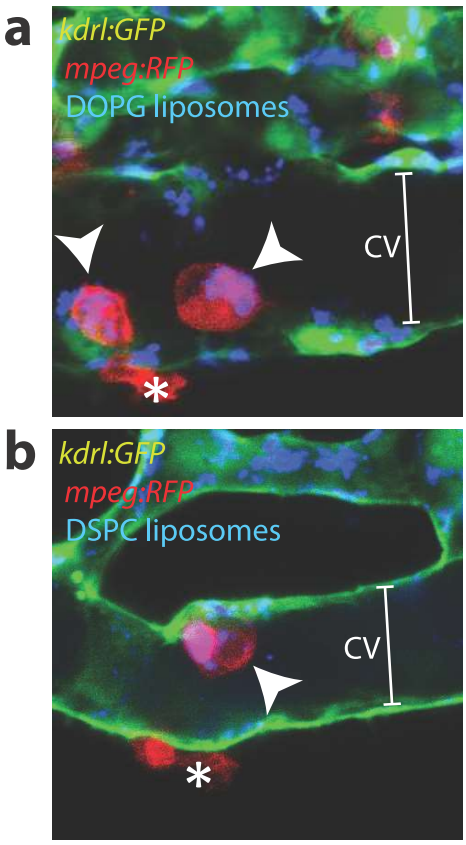
a
kdrl:GFP
mpeg:RFP
DOPG liposomes
CV
b
kdrl:GFP
mpeg:RFP
DSPC liposomes
CV

Figure S6

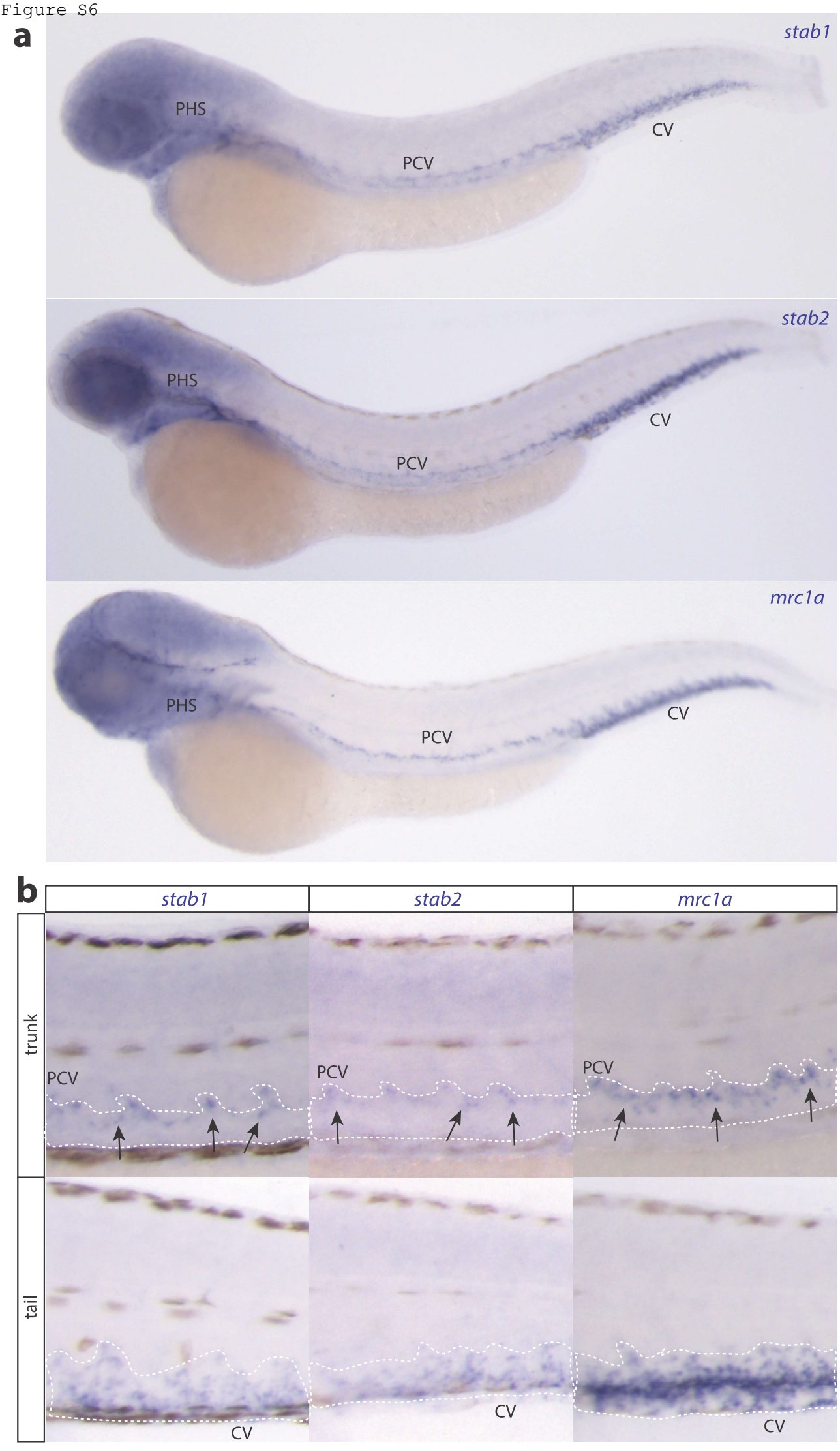
a
stab1
PHS
PCV
CV
stab2
PHS
PCV
CV
mrc1a
PHS
PCV
CV
b
stab1
stab2
mrc1a
trunk
tail
PCV
PCV
PCV
CV
CV
CV

Figure S7

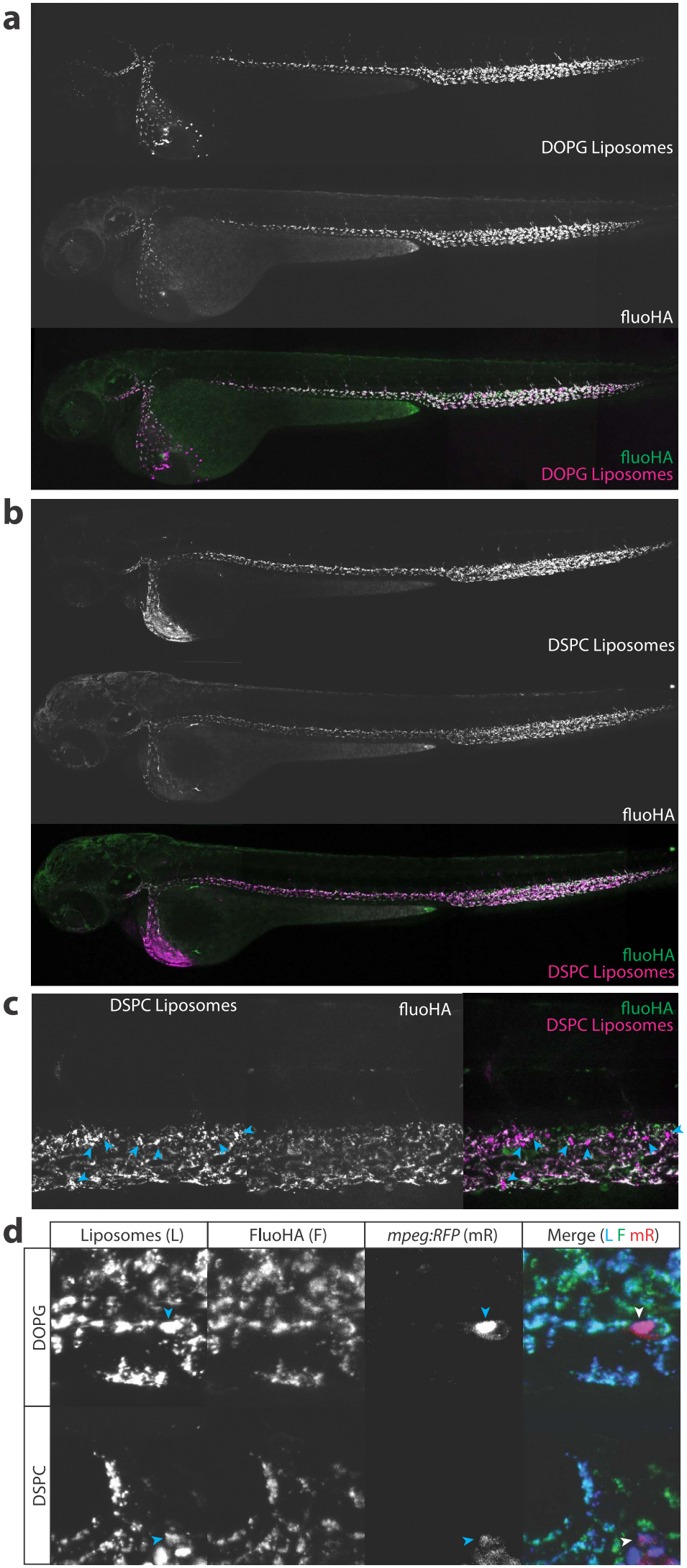
a
DOPG Liposomes
fluoHA
fluoHA
DOPG Liposomes
b
DSPC Liposomes
fluoHA
fluoHA
DSPC Liposomes
c
DSPC Liposomes
fluoHA
fluoHA
DSPC Liposomes
d
Liposomes (L)
FluoHA (F)
mpeg:RFP (mR)
Merge (L F mR)
DOPG
DSPC

Figure S8

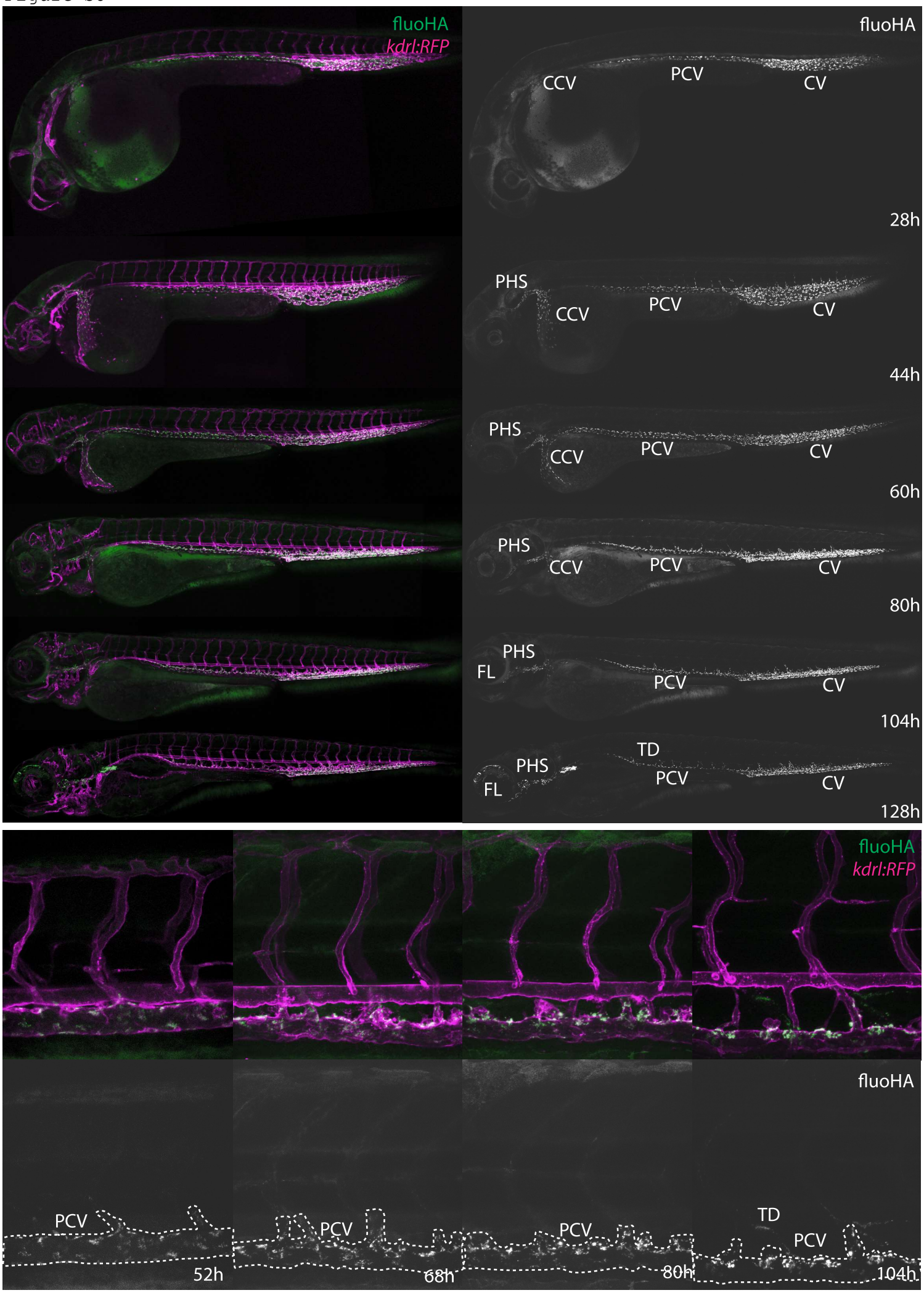
a
fluoHA
kdrl:RFP
fluoHA
CCV
PCV
CV
28h
PHS
CCV
PCV
CV
44h
PHS
CCV
PCV
CV
60h
PHS
CCV
PCV
CV
80h
PHS
FL
PCV
CV
104h
TD
PHS
FL
PCV
CV
128h
b
fluoHA
kdrl:RFP
fluoHA
PCV
52h
PCV
68h
PCV
80h
TD
PCV
104h

Figure S9

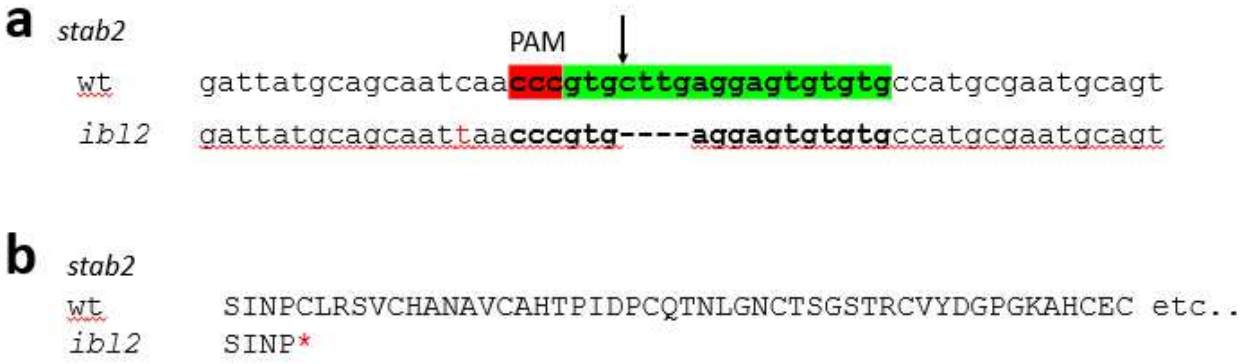
a
stab2
PAM
wt
gattatgcagcaatcaacccgtgcttgaggagtgtgtgccatgcgaatgcagt
ib12
gattatgcagcaattaacccgtg----aggagtgtgtgccatgcgaatgcagt
b
stab2
wt
SINPCLRSVCHANAVCAHTPIDPCQTNLGNCTSGSTRCVYDGPGKAHCEC etc..
ib12
SINP*

Figure S10

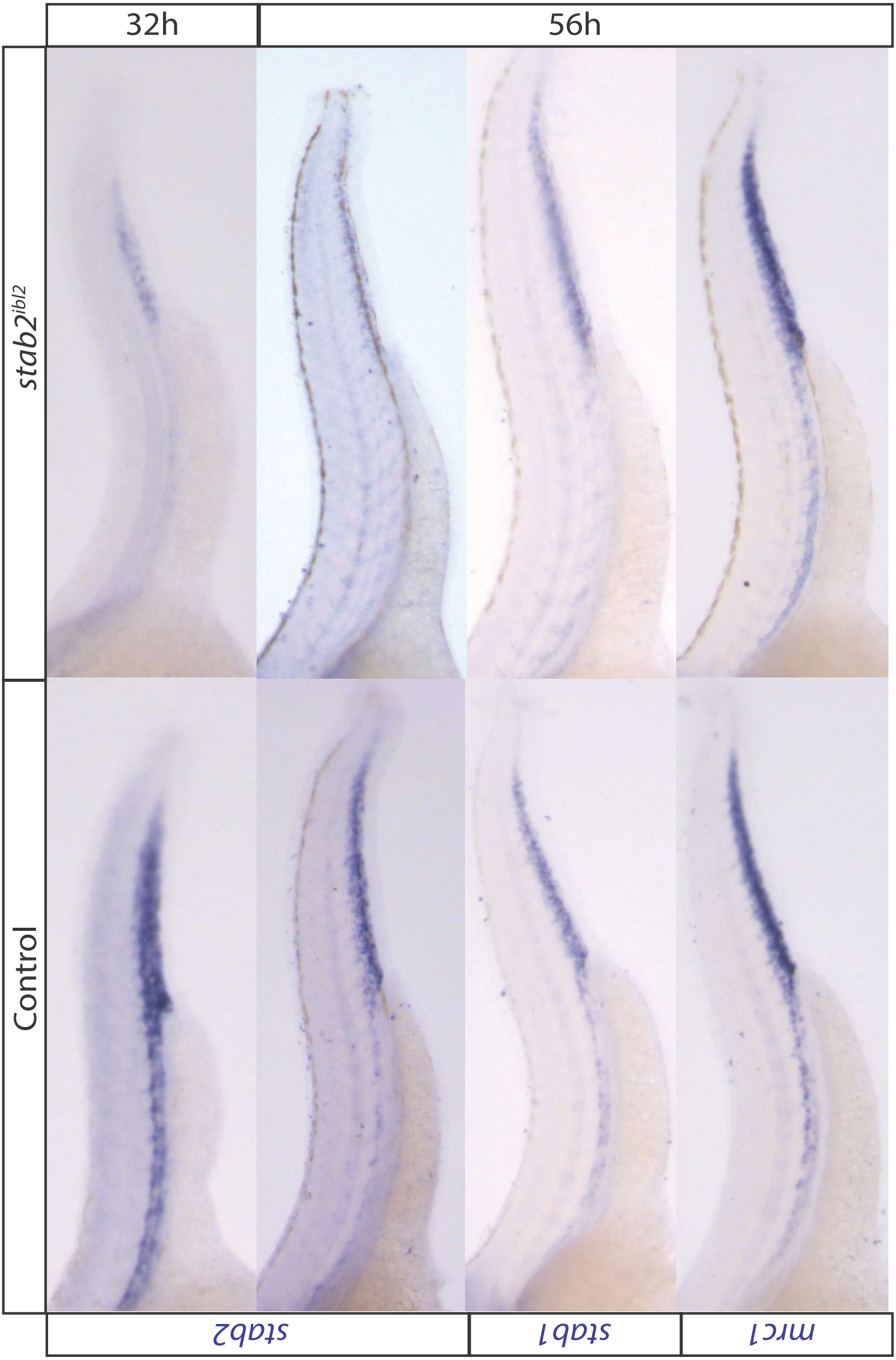

Figure S11

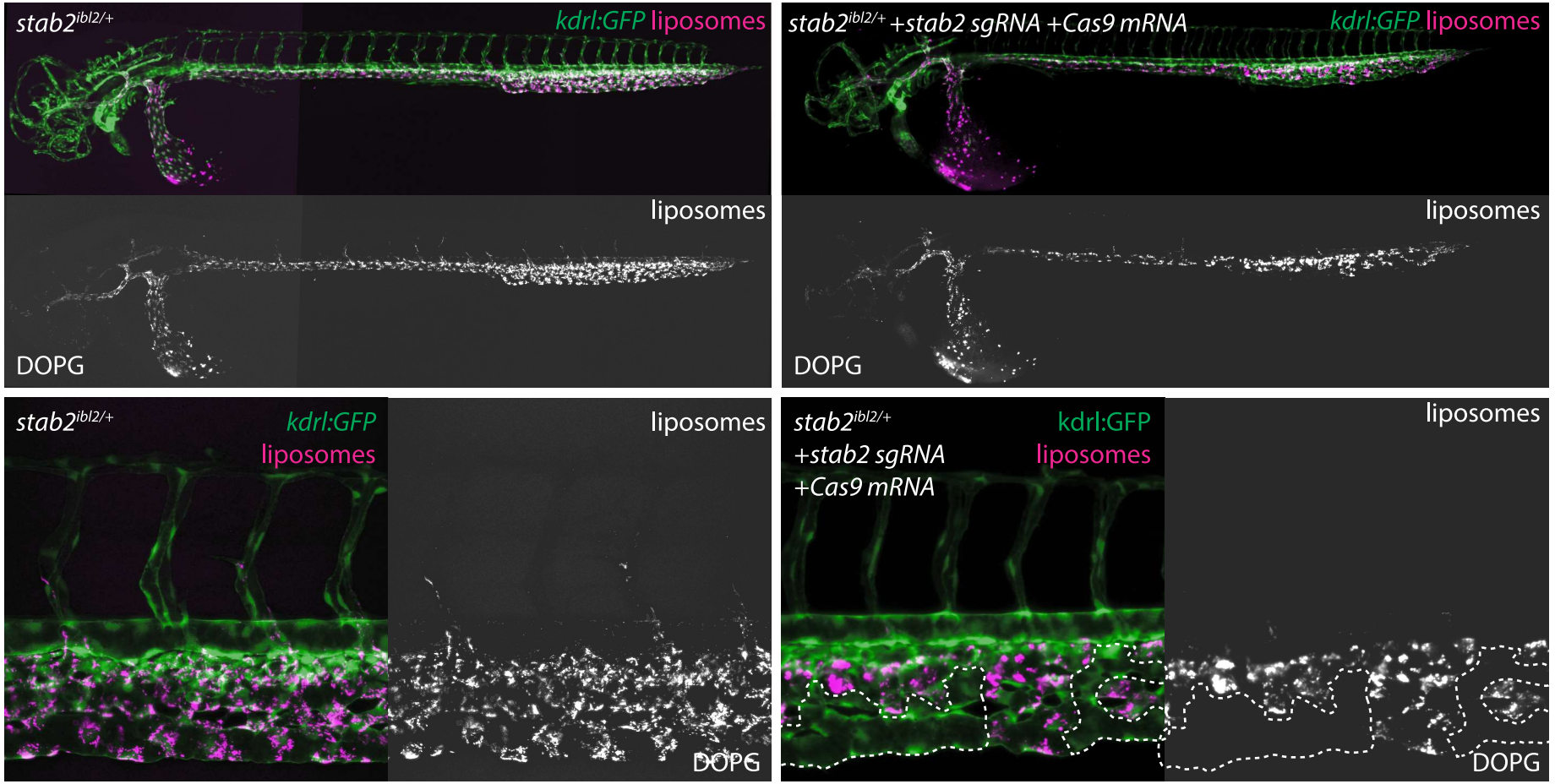
stab2ibl2/+
kdrl:GFP liposomes
liposomes
DOPG
stab2ibl2/+ +stab2 sgRNA +Cas9 mRNA
kdrl:GFP liposomes
liposomes
DOPG
stab2ibl2/+
kdrl:GFP
liposomes
liposomes
DOPG
stab2ibl2/+
+stab2 sgRNA
+Cas9 mRNA
kdrl:GFP
liposomes
liposomes
DOPG

Figure S12

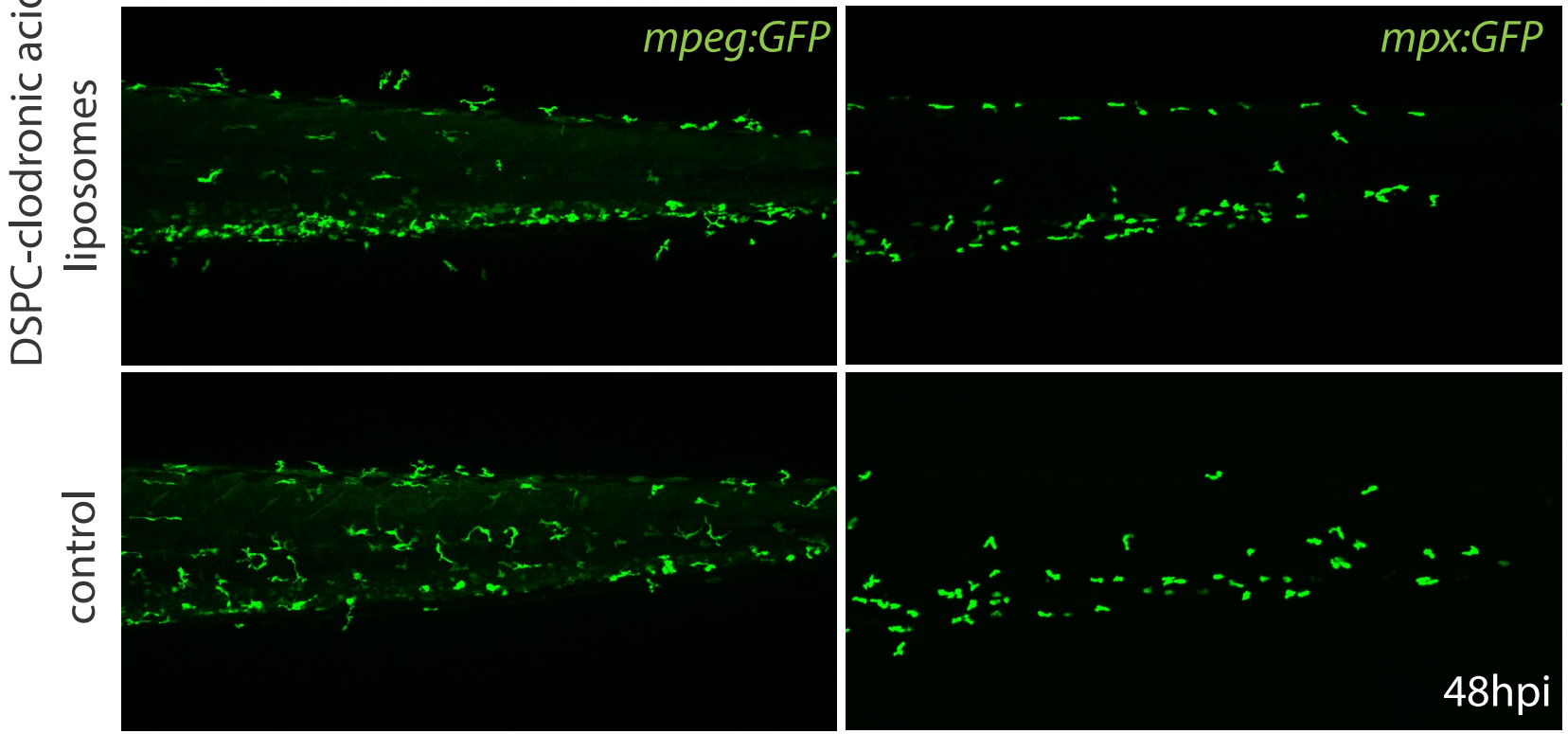
DSPC-clodronic acid liposomes
control
mpeg:GFP
mpx:GFP
48hpi